

High-throughput search for lossless metals

Xiaolei Hu,^{1,2} Zhengran Wu,^{1,2} Zhilin Li,^{1,3,*} Qiunan Xu,⁴ Kun Chen^{①,1,2} Wei Hu,^{1,2} Zhuang Ni^{①,1,2}
 Kui Jin^{①,1,3} Hongming Weng^{①,1,3,†} and Ling Lu^{①,1,3,‡}

¹*Institute of Physics, Chinese Academy of Sciences/Beijing National Laboratory for Condensed Matter Physics, Beijing 100190, China*

²*School of Physical Sciences, University of Chinese Academy of Sciences, Beijing 100049, China*

³*Songshan Lake Materials Laboratory, Dongguan, Guangdong 523808, China*

⁴*Qingdao Institute for Theoretical and Computational Sciences, Shandong University, Qingdao 266237, China*



(Received 21 March 2022; accepted 3 June 2022; published 27 June 2022)

Hypothetical metals having optical absorption losses as low as those of the transparent insulators, if found, could revolutionize optoelectronics. We perform a high-throughput search for lossless metals among all known inorganic materials in the databases of over 100 000 entries. The 381 candidates are identified—having well-isolated partially filled bands—and are analyzed by defining the figures of merit and classifying their real-space conductive connectivity. The superconductor lithium titanate is shown to satisfy the lossless criteria but have a limited bandwidth for low loss. The existing experimental evidence of most candidates being insulating, instead of conducting, is due to the limitation of current density functional theory in predicting narrow-band metals that are unstable against magnetism, structural distortion, or electron-electron interactions. We propose future research directions including conductive oxides, intercalating layered materials, and compressing these false-metal candidates under high pressures into eventual lossless metals.

DOI: [10.1103/PhysRevMaterials.6.065203](https://doi.org/10.1103/PhysRevMaterials.6.065203)

I. INTRODUCTION

Optical photons and electrons, the most important carriers for information and energy, have never been guided efficiently inside the same material due to the high absorption loss of metals. Dielectrics transport photons as in optical fibers and metals conduct electrons as in copper wires. At the photon energy much above that of the lattice phonons, the optical absorption is dominated by the electronic transitions (direct or indirect) between the occupied and empty states. For all existing metals, at any optical frequency, there are always occupied and empty states available for the absorption process to take place [Fig. 1(a)], causing the common misimpression that metals have to be lossy due to the so-called free-carrier absorption.

Fortunately, the carriers in solids are never free electrons, since their density of states (DOS) can be highly modified by the lattice potentials. It is indeed theoretically possible [1,2] for a metal to have zero single-electron transition rate in an energy bandwidth in which the photon absorption can be as low as that in insulators [Fig. 1(b)]. This happens when there is a well-isolated metallic band [of bandwidth W as in Fig. 1(c)] at the Fermi level with a lossless bandwidth of

$$\hbar\Delta\omega = \min\{G_c, G_v\} - W > 0. \quad (1)$$

Equation (1) is the lossless criteria in which the band separation, minimal values of G_c and G_v , have to be larger than

W . G_c and G_v are the energy differences from the Fermi level to the edges of conduction and valence bands. Here, *lossless* means the absence of single-electron absorption—the same sense that insulators are considered lossless below the band gap, where the imaginary part of the dielectric constant ($\epsilon_1 + i\epsilon_2$) vanishes ($\epsilon_2 = 0$). Higher order processes, involving multiple electrons, multiple phonons, and multiple photons, have much lower probabilities and are neglected. This picture of lossless metals was proposed by Medvedeva and Freeman [1] in the context of ideal transparent conductors and by Khurgin and Sun [2] in the context of ideal plasmonic metamaterials. Although electrified [1] and two-dimensional (2D) metals [3] have been suggested as possible directions, lossless metals remain elusive.

The scientific and technological impact of lossless metal is far reaching. For transparent electronics [1,4,5], the inevitable trade-off between conductivity and transmissivity could be broken. For plasmonics [2,3,6] ($\epsilon_1 < 0$), optical devices could be losslessly shrunk to deep subwavelength scales, enhancing light-matter interactions at unprecedented levels [7]. For metamaterials [2,3,6], the numerous remarkable scientific demonstrations, such as cloaking and perfect lens, may deliver practical applications. In reality, even if $\epsilon_1 > 1$ and $\Delta\omega$ is narrow, lossless metals still have exciting consequences, for example, the high material dispersion [8,9] and the waveguiding of both electricity and light. We notice that the three-band configuration of lossless metals is similar to, although having very different requirements than, that of the intermediate-band materials [10], a class of compounds expected to increase the solar-cell efficiency by absorbing a wider spectrum. The field of intermediate-band solar cells also lacks candidate materials [11].

*lizhilin@iphy.ac.cn

†hmweng@iphy.ac.cn

‡linglu@iphy.ac.cn

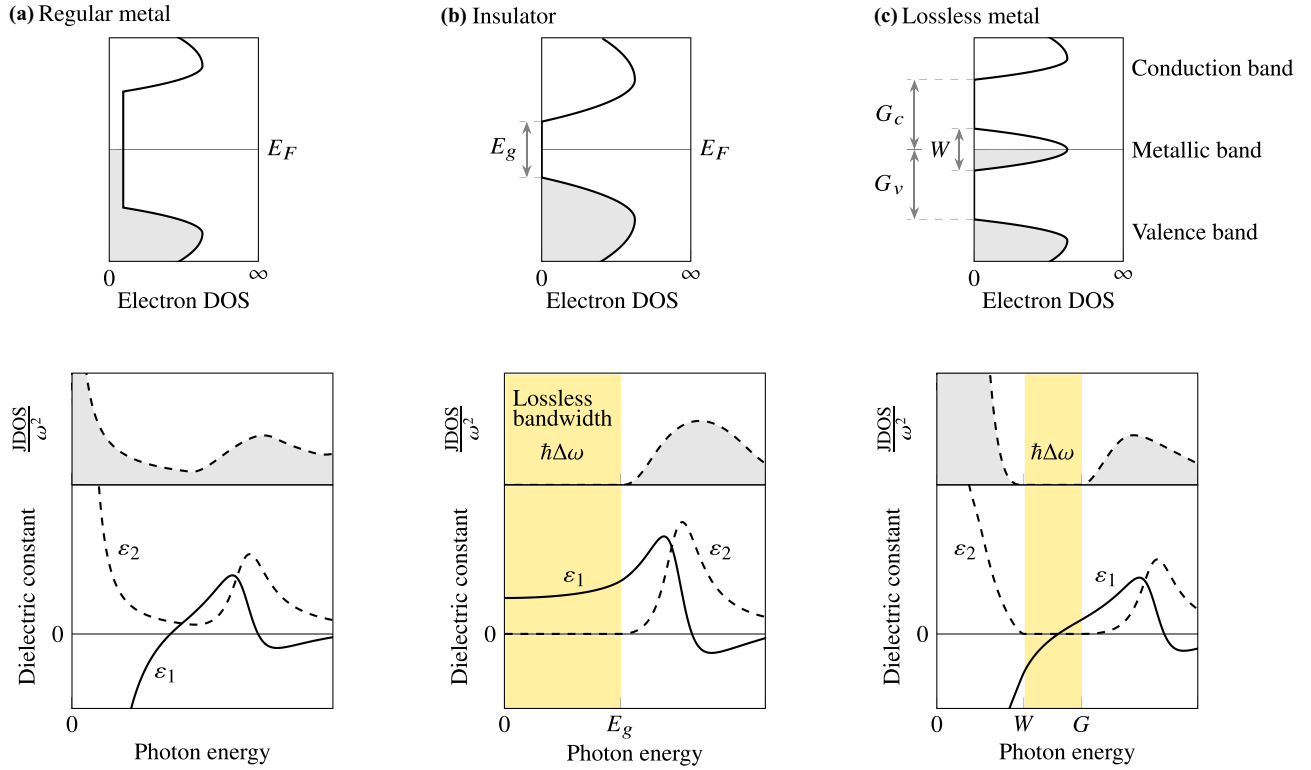


FIG. 1. Comparing lossless metal with regular metal and insulator. (a) Regular metal is lossy across the whole spectrum. (b) Insulator is lossless below the band gap (E_g). (c) Lossless metal, satisfying the lossless criteria ($W < G = \min\{G_c, G_v\}$), has a lossless bandwidth $\hbar\Delta\omega$ from W to G

In the rest of the paper, we first introduce the joint-density-of-states (JDOS) picture [3] for understanding lossless metals. Then, a large-scale computational search is performed to find all potential candidates within the framework of the band theory. The candidates are ranked by the figures of merit (W and $\Delta\omega$) and classified into three classes for their potential conduction paths in the real space. After compiling the previous experimental data on the candidate materials, we identify LiTi_2O_4 , explain the deficiency of current theory in predicting lossless metals, and discuss the next research agenda.

II. JDOS MODEL OF ABSORPTION

The dielectric constant ($\varepsilon_2 = 0$) of a lossless metal cannot be described by the regular Drude model, whose intraband absorption is $\varepsilon_2^{\text{intra}}(\omega) = \frac{\omega_p^2 \Gamma}{\omega(\omega^2 + \Gamma^2)}$, where ω_p is the plasma frequency and Γ is the constant electron scattering rate. It is proposed in Ref. [3] that a frequency-dependent $\Gamma(\omega) \propto \text{JDOS}(\omega)$, with JDOS proportionality, correctly gives $\varepsilon_2 = 0$ inside the lossless bandwidth. The scattering rate is roughly proportional to the JDOS of electrons, because the JDOS captures the phase space of the initial and final states. Here, $\text{JDOS}(\omega) = \int_0^\omega \text{DOS}(\omega' - \omega) \text{DOS}(\omega') d\omega'$ relaxes the momentum conservation to account for the indirect transitions.

Our JDOS-Drude intraband model is

$$\Gamma(\omega) = \frac{\text{JDOS}(\omega)}{\omega \cdot \text{DOS}^2(E_F)} \Gamma_{\text{dc}}, \quad (2)$$

where $\text{DOS}(E_F)$ is the DOS at Fermi energy. At zero frequency, $\Gamma(0) = \Gamma_{\text{dc}} = \epsilon_0 \frac{\omega_p^2}{4\pi} \rho_{\text{dc}}$ (~ 30 THz in silver), in which ρ_{dc} is the measurable resistivity of direct current (dc) and ϵ_0 is the vacuum permittivity. Compared to that in Ref. [3], there is no fitting parameter in our model.

We find that $\varepsilon_2 \propto \text{JDOS}/\omega^2$ can be used as a qualitative estimation of material absorption (as shown in Fig. 1) for both intra- and interband losses. At low frequencies, the intraband loss dominates and $\varepsilon_2^{\text{intra}}(\omega \ll \Gamma_{\text{dc}}) = \frac{\omega_p^2}{\Gamma_{\text{dc}} \text{DOS}^2(E_F)} \text{JDOS}/\omega^2$. At high frequencies, the interband loss dominates and the $\varepsilon_2^{\text{inter}} \propto \text{JDOS}/\omega^2$ scaling is still valid. Because the transition rate, in Fermi's golden rule, is proportional to the vector potential squared $A^2 = (E/\omega)^2$, where E is the electric field [12]. We note that, since the band theory only works in the single-particle regime, it is beneficial to formulate everything using DOS and JDOS that are valid for both interacting and noninteracting electron systems. Equivalently, lossless means zero JDOS.

III. HIGH-THROUGHPUT SEARCH

We search for lossless metals in two computational online material databases of Materials Project [13] and AFLOW [14] with a total of 190 762 material entries (in September 2020) shown in Fig. 2(a). In the main text, we analyze the materials that have experimental relevance—those listed in the Inorganic Crystal Structure Database (ICSD [15]), a comprehensive collection of experimental crystal data. The rest of the materials, not listed in ICSD, are analyzed in

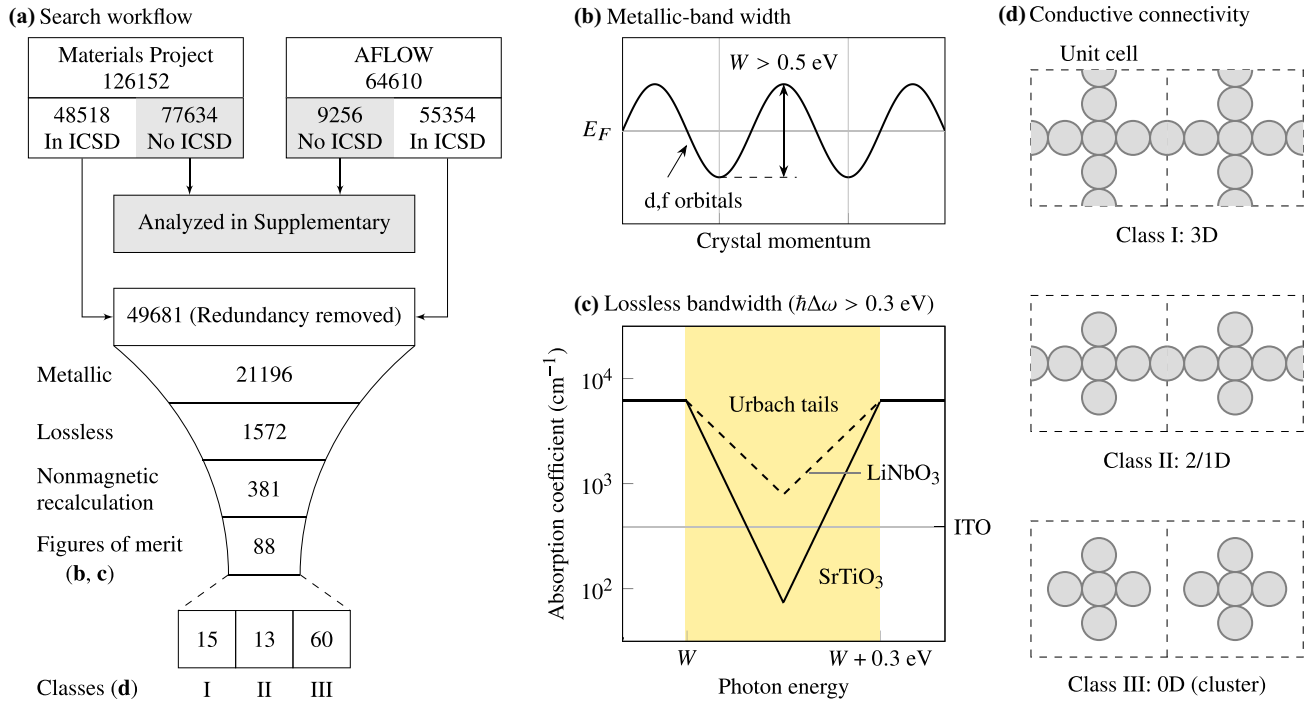


FIG. 2. Search workflow and analysis of lossless-metal candidates. (a) Workflow diagram of the screening steps. All 1572 candidates are listed in the Supplemental Excel file [16]. (b) First figure of merit: the metallic-band width containing d/f orbitals. (c) Second figure of merit: the lossless bandwidth constrained by Urbach absorption tails. (d) The 88 candidates are classified by their real-space conductive connectivity, whether or not the relevant atoms are close enough for current flow.

the Supplemental Material [16]. We focus on the synthesized ICSD materials, because the experimental feedbacks are critical to check the reliability of the theory, without which it is easy to predict fantasy materials [17] that are unstable or not synthesizable. Among the 92 153 ICSD IDs covered in the two databases, there are 49 681 unique compounds after we merge the redundant entries of identical stoichiometries and space groups. The band-structure data are available for 42 729 compounds and 21 196 of them are metals—having partially filled metallic bands at the Fermi levels.

Each band structure in the databases represents a ground state, either magnetic or nonmagnetic, predicted by the density functional theory (DFT) [18,19]. For nonmagnetic ground states, we can directly apply the lossless criteria of Eq. (1) and the energy limit of the search is up to 10 eV. Among the 14 463 nonmagnetic (spin-degenerate) metals, we find 431 lossless-metal candidates. For the rest metals with magnetic ground states (spins splitting), we are actually more concerned about their properties at room temperature (for optical applications) above most magnetic-transition temperatures. In order to estimate their nonmagnetic properties from the available magnetic band structures while keeping enough potential candidates at this step, we relax the lossless criteria to be one of the spin bands satisfying the lossless criteria and obtain 1141 loss-metal candidates. (791 of them satisfy the lossless criteria for both spins.) This spin criteria is justified by the fact that magnetism mostly split the two spins in the band structure.

Aiming at applications under room-temperature where most materials lose their magnetic ordering, we perform

nonmagnetic recalculations for all 1572 candidates (431 nonmagnetic plus 1141 magnetic candidates, which are all listed in the Supplemental Excel file [16]), with improved accuracy, to double check whether they still satisfy the lossless criteria. The high-throughput computations in the databases have compromised settings for speed, while we include the spin-orbit coupling and f orbitals, as well as experimental lattice data from ICSD. Our *ab initio* recalculations are performed using the Vienna *ab initio* simulation package (VASP) with the generalized gradient approximation (GGA) plus Coulomb repulsion (U), detailed in the Supplemental Material [16].

First, we drop the 306 candidates whose chemical formula is in fact different from their ICSD entries. They miss hydrogen atoms in the calculations due to the lack of the hydrogen positions in ICSD. Second, we drop 242 candidates whose DFT calculations do not converge, mostly due to the inclusion of the f orbitals from rare earth elements such as terbium (Tb) and ytterbium (Yb). Third, in the remaining 1024 candidates with correct composition and converging band structures, 637 candidates no longer satisfy the lossless criteria. Our recalculations are more restrictive than the database results for two main reasons. On one hand, the magnetic candidates, from the previous database screening step, are not necessarily lossless for their nonmagnetic band structures. On the other hand, the database band structures are based on the computationally relaxed structures (with GGA DFT), which usually converge to larger lattice constants than the experimental values. An expanded lattice leads to flatter bands so the lossless criteria is more likely to be met. After all, we have 381 lossless-metal candidates left after the nonmagnetic recalculations.

IV. FIGURES OF MERIT

The metallic-band width (W) and lossless bandwidth ($\hbar\Delta\omega$) are the two figures of merit for lossless metals. Larger W usually implies higher mobility and better conductors while larger $\hbar\Delta\omega$ means lower optical absorption.

We remove candidates whose metallic-band width (W) is too narrow to be metals in reality [Fig. 2(b)]. It is well known that a narrow electronic band at Fermi level results in correlation effects (low kinetic energy compared to Coulomb repulsion U) that DFT has a limited predictive power. For example, $W < U$ is considered a condition for Mott insulators, where the U values are on the order of eV listed in the Supplemental Material [16]. This is especially true for d/f orbitals that are intrinsically narrow banded and spatially localized. Sadly, the lossless metal falls right into this category, because a narrow metallic band is required to satisfy the lossless criteria and 355 of the 381 candidates contain d/f orbitals (from transition-metal elements) in their isolated metallic bands. Consequently, we set an empirical lower limit of 0.5 eV on the metallic-band width and remove 229 candidates whose metallic bands are made of d/f electrons and, at the same time, $W < 0.5$ eV. We do not constrain s/p orbitals which are usually handled well by DFT. It is worth noting that, in the case when the metallic band (W) consists of several individually isolated subbands, only the bandwidth of the partially filled isolated subbands are used as the figure of merit.

We also remove candidates whose lossless bandwidth ($\hbar\Delta\omega$) is too narrow to support low optical absorption in reality [Fig. 2(c)]. Although the electron DOS vanishes abruptly at the band edge in a perfectly periodic crystal, real crystals are imperfect and it is well known that the absorption edge drops exponentially with photon energy—the Urbach tails [20,21]. The slope of the tail, reflecting crystal disorder, is quantified by the Urbach energy—a temperature-dependent energy scale across which the absorption coefficient drops by $1/e$. As the temperature drops, the Urbach energy and the optical loss usually decrease, if no phase transition happens in the material. In Fig. 2(c), the room-temperature Urbach energies of two ternary compounds, 34 meV in SrTiO₃ [22] and 78 meV in LiNbO₃ [23], are used to estimate the minimum lossless bandwidth needed to achieve a low enough absorption loss. We do not use the smallest Urbach energies (~ 10 meV) in Si and GaAs, because most other materials could not be grown with such high crystalline qualities. We find that $\hbar\Delta\omega > 0.3$ eV is necessary to realize a lower absorption coefficient than that of the indium tin oxide (ITO [24]), the standard transparent conductor. We note that silver (Ag) might be a better reference than ITO for the wavelengths of negative permittivity. The 0.3 eV lower bound removes 113 candidates (out of 381), including the LiTi₂O₄—a transparent superconductor discussed in a later section.

V. REAL-SPACE ANALYSIS

88 candidates are left with reasonably wide metallic-band width (W) and lossless bandwidth ($\hbar\Delta\omega$). Theoretically, a large $\hbar\Delta\omega$ ensures optical transparency, but a wide W cannot always ensure electrical conduction, because conduction depends more on the real-space wave functions than the

reciprocal-space band dispersions. For example, localized unpaired electrons cannot flow in the lattice, but they appear as “metals” (partially filled bands across the Fermi level) in the band theory (assuming global Bloch modes across the crystal). So we study whether the conductive atoms—the atoms contributing to the electron DOS at the Fermi level (± 50 meV)—are closely spaced enough to connect a current path in the crystal. The connectivity of these conductive atoms is determined by the spatial overlap of their atomic radii [25]. Illustrated in Fig. 2(d), the *conductive connectivity* can be three dimensional (3D), low-dimensional (2D, 1D), or in isolated clusters (0D), according to which we classify the 88 candidates into three classes with 15, 13, and 60 materials, respectively. The candidates of class I, II, and most candidates of class III are tabulated in Table I.

The materials in class I have 3D conductive connectivity (for potential current paths) in vertex-sharing or edge-sharing polyhedrons. The narrow metallic band originates from the localized d/f orbitals. The isolation of the metallic bands is partly due to the large and uniform splitting of the d/f bands in the crystal fields of high symmetries (high space groups). A typical material example is pyrochlore molybdate (Nd₂Mo₂O₇) shown in Fig. 3(a), that is experimentally verified to be a metal (resistance decreases with the decrease of temperature) and is a ferromagnet below the Curie temperature of ~ 90 K [26,27].

The materials in class II have low-dimensional conductive connectivity, in which the atoms connect more closely in one or two dimensions. The weaker coupling in certain directions facilitates bands of less dispersions and narrower bandwidths [3]. A typical example is calcium nickelate CaNi₄O₈ in Fig. 3(b). Nickel dioxide (NiO₂) is a layered insulator having an isolated narrow conduction band (see Supplemental Material [16]). Calcium intercalation, in NiO₂, supplies itinerant electrons and raises the Fermi level into the middle of this narrow conduction band, thus satisfying the lossless-metal criteria. The same mechanism applies to KSnS₂ (detailed in the Supplemental Material [16]), in which potassium intercalates into the tin disulfide (SnS₂)—a common layered material. Neither CaNi₄O₈ [28] nor KSnS₂ [29] have been synthesized in single-crystal forms.

The materials in class III consist of distanced atomic clusters (forming narrow metallic bands), which make it easier, than the other two classes, to satisfy the lossless criteria in DFT calculations. However, the weak couplings between the clusters impede electric conduction. A typical example is the solid oxygen O₂ ($P64/mmc$) in Fig. 3(c), showing a huge lossless bandwidth of $\hbar\Delta\omega = 2.55$ eV with an isolated metallic-band width of $W = 3.17$ eV. This molecular crystal consists of dense arrangement of diatomic molecules under high pressure. In experiments, this phase forms at ~ 17 GPa and is not conducting. The oxygen metallizes under a much higher pressure around 100 GPa [30,31] (see the Supplemental Material [16] for the O₂ phase diagram).

VI. EXISTING EXPERIMENTS

We go through the existing experimental literature on the candidates in Table I and note their key feedback information (the references are listed in the Supplemental Material

TABLE I. Lossless-metal candidates. Top candidates are given for each class, sorted by the lossless bandwidth ($\hbar\Delta\omega$). The experimental references of each material are provided in the Supplemental Material [16]. (T_C/T_N : Curie/Néel temperature of magnetic transition. FM: ferromagnetism. AFM: antiferromagnetism.)

	Formula	Space group	W (eV)	$\hbar\Delta\omega$ (eV)	Conductive connectivity	Magnetism (T_C/T_N) distortion	Color	Conduction
Class I	CoCO ₃	167	0.61	1.95	3D	AFM (18 K)		Insulator
	K ₅ CeCo ₂ (NO ₂) ₁₂	201	0.85	1.70	3D			
	Ba ₂ CoMoO ₆	225	1.12	1.32	3D	AFM (20 K)	Black	
	Sr ₂ CoMoO ₆	225	1.30	1.24	3D	AFM (36 K)	Black	Insulator
	NiMoO ₄	12	0.71	0.91	3D	FM (22 K)	Light green	
	Ba ₂ GdMoO ₆	225	0.93	0.88	3D		Black	Insulator
	KCoF ₃	221	1.67	0.80	3D	AFM (114 K)	Rosy	Insulator
	Nd ₂ Mo ₂ O ₇	227	2.02	0.59	3D	FM (90 K)	Black	Metal
	CoTiO ₃	148	0.74	0.44	3D	AFM (38 K)	Green	Insulator
	CaCr ₂ O ₄	62	1.69	0.42	3D	AFM (43 K)		Insulator
	CaCu ₃ Ti ₄ O ₁₂	204	0.89	0.40	3D	AFM (24 K)		Insulator
	CuSiO ₃	148	1.13	0.37	3D	AFM (110 K)	Black	Insulator
	Li ₂ IrO ₃	70	2.75	0.36	3D	FM (38 K)		Insulator
	Bi ₂ Cu ₅ B ₄ O ₁₄	1	0.90	0.35	3D	FM (25 K)	Green	Insulator
	NiF ₂	58	1.67	0.30	3D	AFM (73 K)		Insulator
LiTi ₂ O ₄	227	2.37	0.12	3D	Superconductor (13.7 K)	Blue	Metal	
Class II	CaNi ₄ O ₈	166	1.33	0.91	2D			
	Sc ₂ Cu ₂ O ₅	33	0.61	0.80	1D	AFM (16 K)		Insulator
	VCl ₃	148	1.19	0.66	2D	FM	Violet	Insulator
	CuZrTiO ₅	19	0.94	0.55	1D	AFM	Green	Insulator
	CuInOPO ₄	62	0.69	0.51	1D		Green	
	Li ₂ CuO ₂	71	1.13	0.48	1D	AFM (9 K)	Brown	Insulator
	BaCu ₂ Si ₂ O ₇	62	0.95	0.42	1D	AFM (9.2 K)	Dark blue	Insulator
	Co ₂ B ₂ O ₅	2	1.55	0.41	1D	AFM (45 K)	Violet	
	Ca ₃ Cu ₅ Si ₉ O ₂₆	15	0.96	0.38	2D		Bluish-green	Insulator
	CsNiBr ₃	194	1.14	0.37	1D	AFM (70 K)	Orange-brown	
	CaCuGe ₂ O ₆	14	0.58	0.36	1D	AFM, Jahn-Teller		Insulator
	Cu(OH)F	14	1.75	0.36	2D	AFM, Jahn-Teller		
	KSnS ₂	166	1.14	0.36	2D			
Class III	NaO ₂	205	0.71	3.57	0D	AFM (193 K)		Insulator
	O ₂	194	3.17	2.55	0D	High-pressure	Dark red	Insulator
	Rb ₄ O ₆	220	0.42	2.44	0D	AFM	Black	Insulator
	LiO ₂	58	1.84	2.28	0D	AFM (7 K)		Insulator
	K ₂ BaCo(NO ₂) ₆	69	1.14	1.61	0D	Jahn-Teller		Insulator
	Nb ₂ (PO ₄) ₃	167	1.16	1.52	0D		Black	Insulator
	Rb ₂ NbCl ₆	225	0.71	1.52	0D	Jahn-Teller		
	RbSb	216	0.96	1.27	0D			Insulator
	K ₂ TaCl ₆	225	0.98	1.03	0D	Jahn-Teller	Black	Insulator
	K ₃ Na(RuO ₄) ₂	15	0.59	0.97	0D	AFM (70 K)	Black	Insulator
	LiBa ₂ Cu ₃ O ₆	69	0.56	0.96	0D	Jahn-Teller		
	Sr ₂ CoWO ₆	225	1.65	0.77	0D	AFM (24 K)	Dark brown	Insulator
	Ba ₂ MgReO ₆	225	1.50	0.75	0D	AFM	Black blue	Insulator
	KRuO ₄	88	0.78	0.74	0D	AFM (150 K)	Black	Insulator
	Cu(HCOO) ₂	14	0.97	0.69	0D	AFM (17 K)	Light blue	Insulator
	SrCu ₂ (BO ₃) ₂	140	0.99	0.59	0D	AFM (1.4 K)	Blue	Insulator
	CuSe ₂ O ₅	15	0.84	0.48	0D	AFM	Green	Insulator
	Ba ₂ CoWO ₆	225	1.93	0.44	0D	AFM (17 K)	Brown	Insulator

[16]). The cold truth is that, experimentally, most candidates are false metals and real insulators [32], except Nd₂Mo₂O₇ (and the LiTi₂O₄ discussed in the next section). The false positive prediction of metals is a common problem of DFT for complex materials involving transition-metal elements, d/f electrons, narrow bands, magnetism, or correlation effects. In reality, these materials usually find insulating ground

states of lower energies, than the predicted metallic states, by structure distortions, magnetic orderings, or electron-electron interactions. As can be seen in Table I, magnetism and cooperative Jahn-Teller distortion are observed for most candidates.

Magnetic orders are difficult to predict. Even the paramagnetic states above the temperatures of magnetic phase

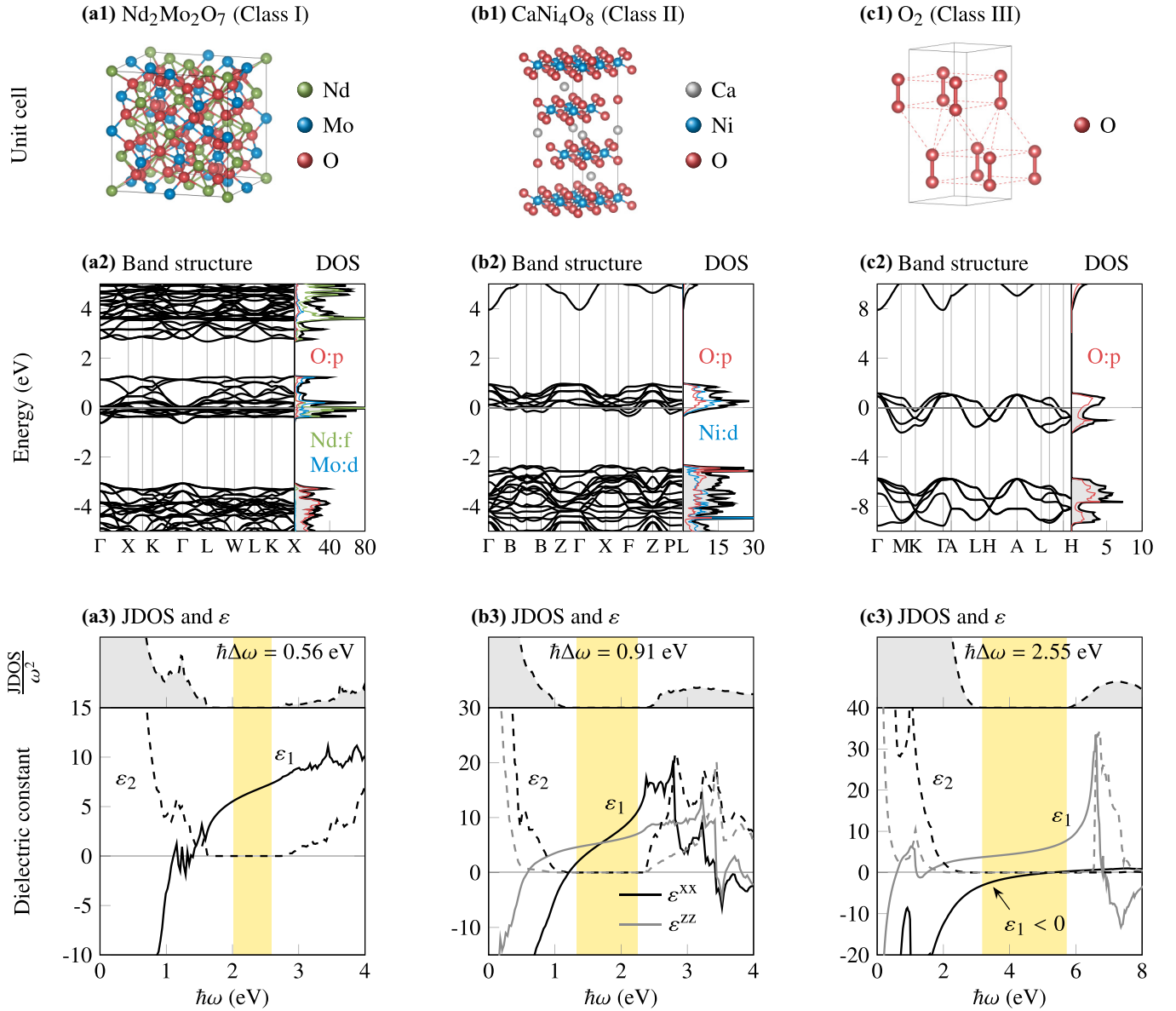


FIG. 3. Three examples of lossless-metal candidates. (a1)–(a3) $\text{Nd}_2\text{Mo}_2\text{O}_7$ ($Fd\bar{3}m$). (b1)–(b3) CaNi_4O_8 ($Fd\bar{3}m$). (c1)–(c3) O_2 ($P64/mmc$). For each material, we plot the crystal structure, band structure, density of states, joint density of states, and dielectric constants. The atomic orbitals that constitute the metallic bands are labeled in (a2)–(c2). Data of the rest candidates are plotted in the Supplemental Material [16].

transitions, containing disordered local magnetic moments, remain a challenge for DFT [32]. So far, our recalculations are nonmagnetic, assuming zero local magnetic moments. The above facts cast doubts on whether more candidates would turn out to be true metals or whether the electronic state of $\text{Nd}_2\text{Mo}_2\text{O}_7$ [Fig. 3(a)] is predicted accurately enough to satisfy the lossless criteria in experiments.

Optical loss is a property that does not have much data in the literature. In most reports, only the sample color is mentioned. But we do require the broadband dielectric constants $\varepsilon(\omega)$, using tools such as the ellipsometry or transmission/reflection, to verify the predictions. Note that the optical absorption (ε_2) is sensitive to the sample quality, so low loss is generally harder to verify experimentally than electric conduction.

VII. LITHIUM TITANATE OF LIMITED LOSSLESS BANDWIDTH

One positive prediction of our search is the spinel lithium titanate shown in Fig. 4. LiTi_2O_4 ($Fd\bar{3}m$) is a well studied metal having a superconducting ground state [33], in contrast to the magnetic orders or structural distortions observed for the false-metal candidates in Table I. Although the bulk single crystal is difficult to grow [34], the thin-film LiTi_2O_4 prepared by the pulsed laser deposition is transparent [35].

We present the experimental optical constants of LiTi_2O_4 in Fig. 4(c). The (100–200 nm) thin film is deposited on MgAl_2O_4 substrate following Ref. [36] and the ellipsometry measurements are performed following Ref. [37]. The LiTi_2O_4 film deteriorates in air and its quality is limited by

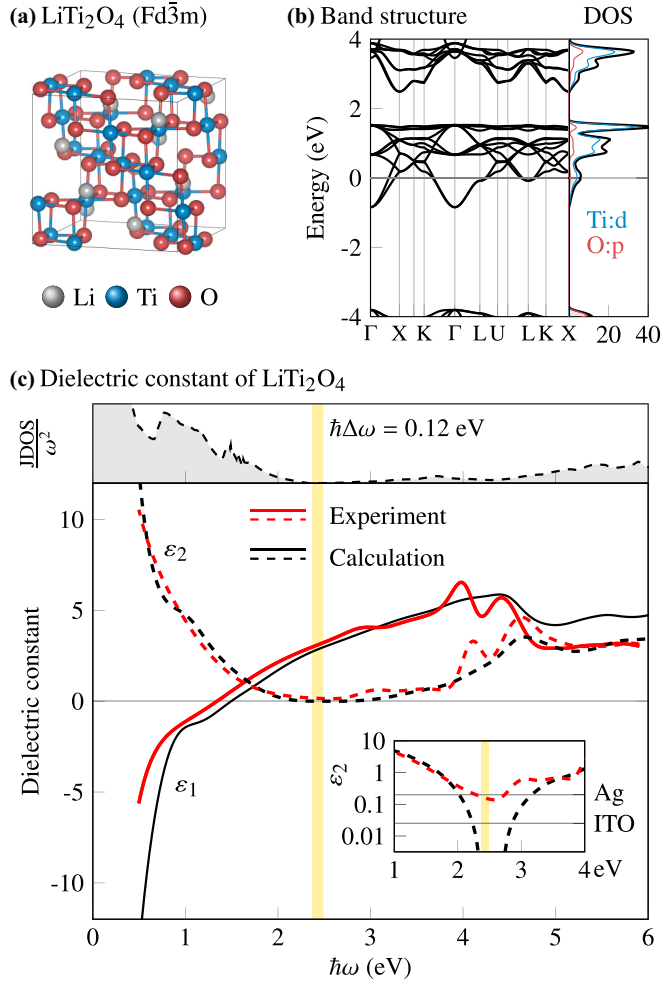


FIG. 4. LiTi_2O_4 with limited lossless bandwidth ($\hbar\Delta\omega = 0.12$ eV). (a) Crystal structure. (b) Band structure and density of states. (c) The experimental and calculated dielectric constants in comparison to the minimum optical loss of silver and indium tin oxide.

the oxygen vacancies present in the sample due to the low oxygen pressure during growth to avoid the insulating phase $\text{Li}_4\text{Ti}_5\text{O}_{12}$ [36].

For LiTi_2O_4 , the agreement between experimental and calculated dielectric constants is encouraging. The minimum loss (ϵ_2) is similar to that of silver, despite its positive ϵ_1 in contrast to the negative ϵ_1 of silver. Unfortunately, the theoretical lossless bandwidth is too narrow ($\hbar\Delta\omega = 0.12$ eV) to support an optical absorption much lower than that of ITO. Nevertheless, if the Fermi level of LiTi_2O_4 could be lowered, the lossless bandwidth will increase and the optical loss could drop quickly.

VIII. FUTURE DIRECTIONS

Although the feedback from existing experiments indicates the drawbacks of the current high-throughput approach in finding lossless metals, the candidates in Table I still serve as reasonable starting points. Efforts should be made to study their failure modes, their actual electronic structures, and their optical properties. These efforts involve *ab initio* calculations

beyond simple DFT [32] such as the dynamical mean-field theory (DMFT), as well as the experimental attempts in growing and characterizing the high-quality single-crystal samples that most of the candidates lack.

The candidates also indicate promising directions for future searches. Obviously, the majority of the entries in Table I are oxides [38]. In class I, transition-metal compounds with high spatial symmetries are promising material systems, for example, the double perovskites (such as $\text{Ba}_2\text{CoMoO}_6$), pyrochlore ($\text{Nd}_2\text{Mo}_2\text{O}_7$), and spinel (LiTi_2O_4). In class II, layered insulators of a narrow band near the Fermi level (such as the SnS_2 and NiO_2 presented in the Supplemental Material [16]) are worth the attention, since their Fermi levels could be tuned by intercalation.

Inspired by the solid oxygen in class III, we propose a high-pressure route to lossless metals. Conceptually, there are two ways to obtain narrow-band metals. One way is expanding the lattice constant of a metal [2] to narrow its bandwidth while maintaining its conduction. However, there is no experimental technique to do that. The other way is shrinking the lattice constant of a false-metal candidate in order to widen its metallic-band width into a metal, through an insulator-metal transition, while maintaining a finite lossless bandwidth. The standard high-pressure technique using diamond-anvil cell is well suited for this purpose, since both the transmission/reflection and the resistance can be monitored when the pressure is applied to the sample [39].

Our current search focuses on the nonmagnetic states, but a large fraction ($\sim 34\%$) of the database entries are predicted to have magnetic ground states, whose nonmagnetic band structures are unavailable. So our magnetic spin criteria could miss some of the nonmagnetic candidates due to the lack of nonmagnetic band structures in the databases. Since magnetism plays an important role in narrow-band systems and at low temperatures, magnetic lossless metals are worth more careful considerations.

IX. CONCLUSION

We perform a high-throughput screening for the elusive lossless metals. Starting from 44 660 distinctive inorganic materials in ICSD, we obtain 88 high-quality candidates, while most of them are found to be insulating in experiments. As an encouraging example, the optical absorption of LiTi_2O_4 is shown to be limited by the small lossless bandwidth. Lossless metals are difficult to predict using the current condensed-matter theory due to the complexity of the candidate material systems, so that the experimental efforts are highly encouraged. Nevertheless, our results shine light on a few hopeful directions including oxide conductors, low-dimensional metals, and compressing the false-metal candidates. Finally, we emphasize that our current search is far from complete, because the data quantity and accuracy in the databases are still under development. The search could also be extended to organic materials.

ACKNOWLEDGMENTS

This work is supported by the Chinese Academy of Sciences through the Youth Innovation Promotion

Association (Grant No. 2021008), the Project for Young Scientists in Basic Research (Grant No. YSBR-021), the Strategic Priority Research Program (Grant No. XDB33000000), the Informatization Plan (Grant No. CAS-WX2021SF-0102), the Interdisciplinary Innovation Team, and the International Partnership Program with the Croucher Foundation (Grant No. 112111KYSB20200024),

by the National Key R&D Program of China (Grants No. 2017YFA0303800, No. 2017YFA0303800, and No. 2018YFA0305700), by the Natural Science Foundation of China (Grants No. 12025409, No. 11721404, No. 11974415, No. 12025409, No. 11721404, No. 11974415, No. 11925408, No. 11921004, and No. 12188101), and by Beijing Natural Science Foundation (Grant No. Z200008).

-
- [1] J. E. Medvedeva and A. J. Freeman, Combining high conductivity with complete optical transparency: A band structure approach, *Europhys. Lett.* **69**, 583 (2005).
- [2] J. B. Khurgin and G. Sun, In search of the elusive lossless metal, *Appl. Phys. Lett.* **96**, 181102 (2010).
- [3] M. N. Gjerding, M. Pandey, and K. S. Thygesen, Band structure engineered layered metals for low-loss plasmonics, *Nat. Commun.* **8**, 15133 (2017).
- [4] X. Zhang, L. Zhang, J. D. Perkins, and A. Zunger, Intrinsic Transparent Conductors without Doping, *Phys. Rev. Lett.* **115**, 176602 (2015).
- [5] G. Brunin, F. Ricci, V.-A. Ha, G.-M. Rignanese, and G. Hautier, Transparent conducting materials discovery using high-throughput computing, *npj Comput. Mater.* **5**, 63 (2019).
- [6] J. B. Khurgin and A. Boltasseva, Reflecting upon the losses in plasmonics and metamaterials, *MRS Bull.* **37**, 768 (2012).
- [7] O. D. Miller, A. G. Polimeridis, M. T. H. Reid, C. W. Hsu, B. G. DeLacy, J. D. Joannopoulos, M. Soljačić, and S. G. Johnson, Fundamental limits to optical response in absorptive systems, *Opt. Express* **24**, 3329 (2016).
- [8] J. B. Khurgin, Expanding the photonic palette: Exploring high index materials, *ACS Photon.* **9**, 743 (2022).
- [9] H. Shim, F. Monticone, and O. D. Miller, Fundamental limits to the refractive index of transparent optical materials, *Adv. Mater.* **33**, 2103946 (2021).
- [10] A. Luque and A. Martí, Increasing the Efficiency of Ideal Solar Cells by Photon Induced Transitions at Intermediate Levels, *Phys. Rev. Lett.* **78**, 5014 (1997).
- [11] D. JR. Baquiao and G. M. Dalpian, Computational screening of bulk materials with intrinsic intermediate band, *Comput. Mater. Sci.* **158**, 382 (2019).
- [12] G. Grosso and G. P. Parravicini, *Solid State Physics* (Academic Press, New York, 2013).
- [13] <https://materialsproject.org>.
- [14] <http://afLOW.org>.
- [15] <https://icsd.fiz-karlsruhe.de>.
- [16] See Supplemental Material at <http://link.aps.org/supplemental/10.1103/PhysRevMaterials.6.065203> for non-ICSD search results, material references, and examples of more candidates.
- [17] A. Zunger, Beware of plausible predictions of fantasy materials, *Nature (London)* **566**, 447 (2019).
- [18] A. Jain, G. Hautier, C. J. Moore, S. P. Ong, C. C. Fischer, T. Mueller, K. A. Persson, and G. Ceder, A high-throughput infrastructure for density functional theory calculations, *Comput. Mater. Sci.* **50**, 2295 (2011).
- [19] S. Curtarolo, W. Setyawan, G. L. W. Hart, M. Jahnatek, R. V. Chepulskii, R. H. Taylor, S. Wang, J. Xue, K. Yang, O. Levy *et al.*, AFLOW: An automatic framework for high-throughput materials discovery, *Comput. Mater. Sci.* **58**, 218 (2012).
- [20] F. Urbach, The long-wavelength edge of photographic sensitivity and of the electronic absorption of solids, *Phys. Rev.* **92**, 1324 (1953).
- [21] S. S. Mitra and B. Bendow, *Optical Properties of Highly Transparent Solids* (Plenum, New York, 1975).
- [22] D. Goldschmidt and H. L. Tuller, Fundamental absorption edge of SrTiO₃ at high temperatures, *Phys. Rev. B* **35**, 4360 (1987).
- [23] R. Bhatt, I. Bhaumik, S. Ganesamoorthy, A. K. Karnal, M. K. Swami, H. S. Patel, and P. K. Gupta, Urbach tail and bandgap analysis in near stoichiometric LiNbO₃ crystals, *Phys. Status Solidi A* **209**, 176 (2012).
- [24] T. A. F. König, P. A. Ledin, J. Kerszulis, M. A. Mahmoud, M. A. El-Sayed, J. R. Reynolds, and V. V. Tsukruk, Electrically tunable plasmonic behavior of nanocube-polymer nanomaterials induced by a redox-active electrochromic polymer, *ACS Nano* **8**, 6182 (2014).
- [25] J. C. Slater, Atomic radii in crystals, *J. Chem. Phys.* **41**, 3199 (1964).
- [26] I. Kézsmárki, N. Hanasaki, D. Hashimoto, S. Iguchi, Y. Taguchi, S. Miyasaka, and Y. Tokura, Charge Dynamics Near the Electron-Correlation Induced Metal-Insulator Transition in Pyrochlore-Type Molybdates, *Phys. Rev. Lett.* **93**, 266401 (2004).
- [27] I. Kézsmárki, S. Onoda, Y. Taguchi, T. Ogasawara, M. Matsubara, S. Iguchi, N. Hanasaki, N. Nagaosa, and Y. Tokura, Magneto-optical effect induced by spin chirality of the itinerant ferromagnet Nd₂Mo₂O₇, *Phys. Rev. B* **72**, 094427 (2005).
- [28] P. N. Bityutskii and V. I. Khitrova, Electron-diffraction investigation of the crystal structures of anhydrous alkaline-earth (Ca, Sr, Ba) nickelates, *Sov. Phys. Crystallogr.* **29**, 270 (1984).
- [29] M. Bronold, C. Pettenkofer, and W. Jaegermann, Alkali metal intercalation into SnS₂, *Appl. Phys. A* **52**, 171 (1991).
- [30] Y. Akahama, H. Kawamura, D. Häusermann, M. Hanfland, and O. Shimomura, New High-Pressure Structural Transition of Oxygen at 96 GPa Associated with Metallization in a Molecular Solid, *Phys. Rev. Lett.* **74**, 4690 (1995).
- [31] K. Shimizu, E. MI, K. Suhara, and K. Amaya, Oxygen under high pressure-temperature dependence of electrical resistance, *Rev. High Press. Sci. Technol.* **7**, 784 (1998).
- [32] O. I. Malyi and A. Zunger, False metals, real insulators, and degenerate gapped metals, *Appl. Phys. Rev.* **7**, 041310 (2020).
- [33] D. C. Johnston, H. Prakash, W. H. Zachariasen, and R. Viswanathan, High temperature superconductivity in the Li-Ti-O ternary system, *Mater. Res. Bull.* **8**, 777 (1973).
- [34] C. Chen, M. Spears, F. Wondre, and J. Ryan, Crystal growth and superconductivity of LiTi₂O₄ and Li_{1+1/3}Ti_{2-1/3}O₄, *J. Cryst. Growth* **250**, 139 (2003).
- [35] A. Kumatani, T. Ohsawa, R. Shimizu, Y. Takagi, S. Shiraki, and T. Hitosugi, Growth processes of lithium titanate thin films

- deposited by using pulsed laser deposition, *Appl. Phys. Lett.* **101**, 123103 (2012).
- [36] Y. Jia, G. He, W. Hu, H. Yang, Z. Yang, H. Yu, Q. Zhang, J. Shi, Z. Lin, J. Yuan *et al.*, The effects of oxygen in spinel oxide $\text{Li}_{1+x}\text{Ti}_{2-x}\text{O}_{4-\delta}$ thin films, *Sci. Rep.* **8**, 3995 (2018).
- [37] M. Zhao, J. Lian, Y. Jia, K. Jin, L. Xu, Z. Hu, X. Yang, and S. Kang, Investigation of the optical properties of LiTi_2O_4 and $\text{Li}_4\text{Ti}_5\text{O}_{12}$ spinel films by spectroscopic ellipsometry, *Opt. Mater. Express* **6**, 3366 (2016).
- [38] N. Tsuda, K. Nasu, A. Fujimori, and K. Siratori, *Electronic Conduction in Oxides* (Springer Science & Business Media, New York, 2000), Vol. 94.
- [39] A. Jayaraman, Diamond anvil cell and high-pressure physical investigations, *Rev. Mod. Phys.* **55**, 65 (1983).